Journal of Thermal Analysis and Calorimetry, Vol. 81 (2005) 417–423

THERMAL ANALYSIS STUDY OF $Bi_2Sr_2Ca_2Cu_{3-x}Er_xO_{10+\delta}$ GLASS–CERAMIC SYSTEM

M. A. Aksan[*]*, M. E. Yakinci and Y. Balci*

İnönü Üniversitesi, Fen Edebiyat Fakültesi, Fizik Bölümü, 44069 Malatya, Turkey

We have fabricated glasses in the Bi-2223 HT_c superconductor system with $Bi_2Sr_2Ca_2Cu_{3-x}Er_xO_{10+\delta}$ nominal composition, where x=0.5 and 1.0, by the glass-ceramic technique. Using an analysis developed for non-isothermal crystallization studies, information on some aspects of crystallization temperature and thermal properties has been obtained. The crystallization studies were made using DTA with several uniform rates. The calculations of crystallization activation energies, E_a, and the Avrami parameters, n, were made based on the non-isothermal kinetic theory of Kissinger and the Ozawa's equations. The DTA data of the samples showed that the first crystallization temperature, T_{x1}, increases and the second crystallization temperature, T_{x2}, decreases by increasing the Er concentration. This suggests that the Er substitution had significant effect on the glassification of the BSCCO material due to change on the surface nucleation and increased ionic activities at high temperature region. The activation energy for crystallization, E_a, of the samples was also showed an increase at high Er concentration case. However, the Avrami parameter, n, decreased from 2.5 to 1.7 for x=0.5 and 1.0 samples, respectively. This suggests that the growth mechanism is diffusion-controlled and three-dimensional parabolic growth takes place near the first crystallization temperature. The oxidization rates and the activation barrier for oxygen out-diffusion process, E, was calculated using the TG data. It was found that the total mass gain in the x=0.5 sample is comparably smaller than that of the x=1.0 sample. This shows that the oxygen absorption of the x=1.0 sample is faster than the x=0.5 sample, leading to increase in the oxidization rate in the x=1.0 material.

Keywords: *Avrami parameter, crystallization activation energy, DTA, HT_c superconductivity, oxidization rates, oxygen out-diffusion process, TG*

Introduction

Glasses (super-cooled liquids) are very convenient for fundamental studies of the diffusion process and atomic rearrangement, which control the nucleation and crystal growth. The development of many crystal types including meta-stable and stable phases and the formation of solid solution phases can be investigated under controlled conditions. Because some of the molten glasses are very good solvents for many oxides and compounds, the effect of these present as minor constituents upon crystal nucleation and growth process can be investigated. In addition, they have technological importance and advantages with respect to shaping and continuous processing if they can be processed in an appropriate viscosity range. Today there is a wide range of technological applications such as electrical, magnetic, thermal and optical devices and use of coating for metal surfaces, so growing interest in these solids produces many new studies and materials related with the glasses [1–17].

One of the important topics in glass technology is the crystallization of the glass materials. The crystal growth in glasses is controlled either by the rate of aggregation of the structural units to the crystal lattice or by diffusion. First case applies when the glass composition does not change during crystallization, i.e.; the crystal growth rate is constant with time. The second is characterized by the modification of the glass composition with a rate, function of the square root of time. However, when the scale of the diffusion field becomes constant, the growth rate can be time independent even for diffusion-controlled growth.

Isothermal and non-isothermal experimental techniques provide many advantages to investigate glass-crystal transformation. While phase transformations occur too rapidly to be measured isothermal conditions because of transients inherently associated with the experimental apparatus, industrial process depends on the kinetic behavior of systems undergoing phase transformation under non-isothermal conditions. Therefore, a definitive measurement of non-isothermal transformation kinetics is desirable.

Thermoanalytical techniques such as differential thermal analysis (DTA), differential scanning calorimetry (DSC) and thermogravimetric analysis (TG) is widely used experimental techniques to investigate the kinetics of non-isothermal nucleation and growth transformation. Most popular thermal analysis method for studies of the crystallization of glass materials was

* Author for correspondence: maksan@inonu.edu.tr

1388–6150/$20.00

Akadémiai Kiadó, Budapest, Hungary
Springer, Dordrecht, The Netherlands

developed by Kissinger [18], in which second derivative of the fractional crystallization with respect to time is taken as zero and the kinetic parameters were determined from the graph of the logarithm of the temperature squared at the maximum of the reaction rate *vs*. the reciprocal of the temperature in non-isothermal experiments.

Recently, HT_c superconductor materials have joined the new application areas of glass ceramics. It was found that some of the new HT_c copper oxide superconducting materials have a large glass formation range of composition, particularly the $Bi_2Sr_2Ca_{n-1}Cu_nO_{2n+4+\delta}$ (where n=1, 2 and 3) system [19]. The glass-ceramic form of the BSCCO HT_c superconducting system has been fabricated and investigated by many groups. Materials produced with conventional glass-ceramic method may offer many advantages and in some cases yield better properties than the ordinary solid-state ceramic technique. For example; essential points for HT_c superconductor materials, such as pore-free, highly dense, homogeneous structure with strong grain connection and shapability can easily be achieved. However, to achieve good superconducting properties, the thermal properties of the BSCCO material must be taken into account carefully. Particularly, substitution and/or doping to the BSCCO material can be effective on the thermal properties and so directly on the formation of the necessary superconducting crystal growth.

The thermal analysis studies in BSCCO glass-ceramic system have been worked by many research groups [14–17, 20–31]. DTA, DSC and TG properties have been widely investigated and crystallization kinetics, crystallization activation energy and Avrami parameter have been calculated. However, oxidization rates of the BSCCO glass material, which is important for advance crystallization properties and also effect of Er substitution on the thermal properties, have not been investigated widely.

In this study, the Er substituted $Bi_2Sr_2Ca_2Cu_{3-x}Er_xO_{10+\delta}$ high-T_c system (where x=0.5 and 1.0) has been prepared by conventional glass-ceramic technique for the first time. Therefore, we focused on the thermal properties (DTA and TG) of the materials prepared, crystallization kinetics and the oxidization rates were computed by using DTA and TG data.

Experimental

High-purity (99.99%) powders of Bi_2O_3, $SrCO_3$, $CaCO_3$, CuO and Er_2O_3 were used to prepare a nominal composition $Bi_2Sr_2Ca_2Cu_{3-x}Er_xO_{10+\delta}$, where x=0.5 and 1.0. Powders were mixed in agate mortar for 3 h to obtain homogeneous mixture of each composition. The mixture was melted between 1050–1250°C, depending on the composition, in air for 30 min in an α-alumina (Al_2O_3) crucible. The molten materials were quenched quickly between two cold copper plates. Thus, dark, shiny and approximately 3 mm thick glass samples were obtained.

Crystallization studies were performed under non-isothermal conditions using DTA based non-isothermal kinetic theory and samples were heated using four different uniform heating rates (α=5, 10, 20 and 30°C min^{-1}). DTA analyses were performed with a Shimadzu thermal analysis network system 60 with α-alumina reference material. The glass transition temperature, T_g, and crystallization temperatures, T_x, were obtained directly from the DTA results. The crystallization activation energy, E_a, and the Avrami parameter, n, of each composition were calculated using Kissinger method and the Ozawa's equation, respectively.

The TG measurements were carried out using a Shimadzu TGA-50 thermogravimetric analyzer. All the scans were recorded between 200–750°C at a heating rate of 10°C min^{-1} under O_2 atmosphere and mass gain and loss of the materials were measured as a function of temperature. The oxidization rates and the activation barrier for oxygen out-diffusion process, E, was calculated using the TG data.

Results and discussion

DTA results

The DTA results from the x=0.5 and x=1.0 materials are shown in Figs 1 and 2, respectively and also in Table 1. The DTA traces of both compositions showed an endothermic activity between 487 and 494°C, which is known as a glass transition temperature, T_g. For x=0.5 samples, two exothermic peaks were obtained just after the glass transition temperature at all heating rates, Fig. 1. The first peak at around 500°C is believed to be due to the nucleation assisted first crystallization temperature, T_{x1}. The second peak between 540 and 558°C (depending on the heating rate) can be due to the formation of low temperature impurity phases, such as Cu–Er or Bi–Ca contained impurity phases.

The third exothermic peak after 770°C, T_{x3}, could be due to crystallization of the Bi-2212 phase of the BSCCO system either by reaction between the low temperature impurity phases or directly from the residual glassy phase at this temperature. For different compositions of BSCCO glass materials, similar exothermic activities were found previously by many other research groups [15–17, 21].

In the case of x=1.0 sample, the thermodynamic activities was found to be different than that of the x=0.5 sample. Three exothermic peaks were obtained for slow heating rates, Fig. 2. However, for fast heating rate, α=30°C min^{-1}, only two exothermic activities

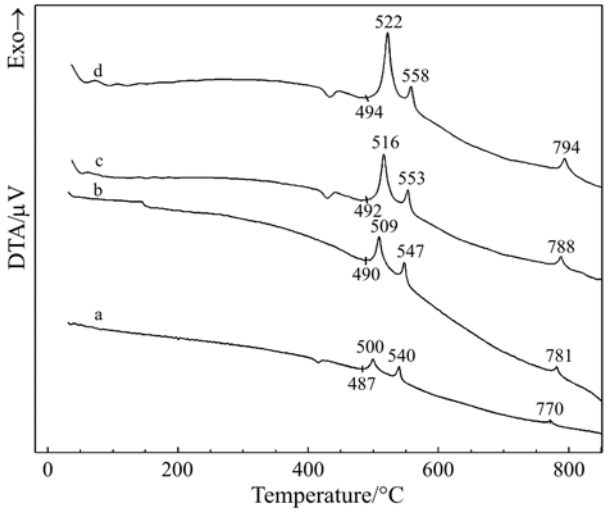

Fig. 1 DTA plots of the x=0.5 sample at different heating rates, α, a – α=5°C min^{-1}, b – α=10°C min^{-1}, c – α=20°C min^{-1} and d – α=30°C min^{-1}

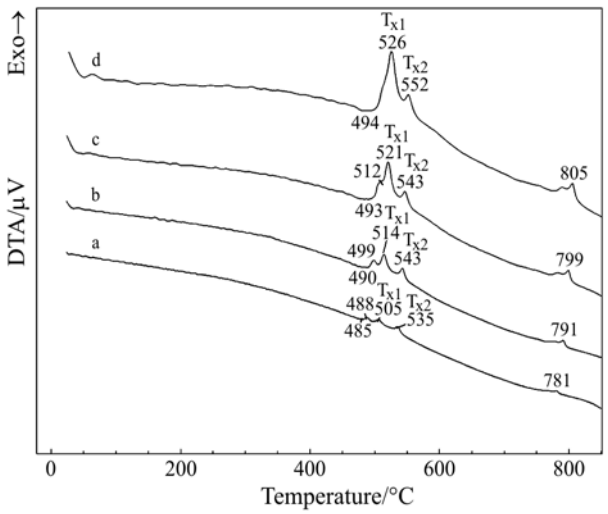

Fig. 2 DTA plots of the x=1.0 sample at different heating rates, α, a – α=5°C min^{-1}, b – α=10°C min^{-1}, c – α=20°C min^{-1} and d – α=30°C min^{-1}

were found to be visible, but the third peak believed to be overlapped by the other two peaks, Fig. 2d. We believed that the first peaks appeared at 488, 499 and 512°C, (Figs 2a, b and c) that is not visible in the DTA patterns of the x=0.5 samples, corresponds to the enlarged nucleation centers by the Er substitution. The other peaks, T_{x1} and T_{x2}, obtained after 488, 499 and 512°C, Figs 2a, b and c, is attributed to the formation of the impurity phases. The third exothermic peak, T_{x3}, obtained between 781 and 805°C, depending on the heating rate, could be due to crystallization of the Bi-2212 phase of the BSCCO system.

In general, shift of T_{x1} to the high temperature region by increasing the heating rate depends on the nucleation rate of the Bi-2212 material. In the case of the rapid heating rate, especially for the α=20 and 30°C min^{-1}, the material stays in the temperature region of nucleation for a time shorter than the time lag. Although when the heating rate is low, the samples stay in the temperature region of nucleation for times longer than time lag and the formation of secondary nuclei might take place [32]. In addition, an increase on the T_{x1} reveals the increase in the surface nucleation in the materials [20].

It was also observed that the first crystallization temperature of the samples, T_{x1}, shows an increase but the T_{x2} exhibited a decrease by increasing the Er concentration in the BSCCO system. This indicates a strong dependence to the substitution level. That is important in controlling the growth mechanism of the BSCCO glass-ceramic system and suggested that the thermodynamic activity of the ions increases when the Er concentration increases to high levels. Therefore, the phase coherence and thermodynamic properties of the x=1.0 system was changed and consequently Cu–Er or Bi–Ca rich impurity phases were formed at low temperature regions. This kind of behavior suggests that the glasses in the stable condition accept the ions only within a limited concentration value. For the substitution of the ions below and/or above this limit, the system does not come into thermodynamically stable condition easily and so temperature range of the thermodynamically stable condition can be changed comparing with the unsubstituted materials [14, 15].

Formation of the new exothermic peak just before the T_{x1} in the x=1.0 sample, Figs 2a, b and c, is believed to be due to the large nucleation centers that occurs initially on the surface of the samples and then it is con-

Table 1 The DTA data of the samples prepared

Material x	Heating rate, α/°C min^{-1}	T_g/°C	T_{x1}/°C	T_{x2}/°C	T_{x3}/°C	ΔT (T_{x1}–T_g)/°C
0.5	5	487	500	540	770	13
	10	490	509	547	781	19
	20	492	516	553	788	24
	30	494	522	558	794	28
1.0	5	485	505	535	781	20
	10	490	514	542	791	24
	20	493	521	546	799	28
	30	494	526	552	805	32

verted rapidly to a crystalline form. The substitution of Er in the BSCCO system was also found to be effective on the glass working range, $\Delta T=(T_{x1}-T_g)$, that is a measure of the stability of the glass phase. The ΔT increases when the concentration of Er increases, this obviously indicates that the Er substitution would retain glass-forming ability in the BSCCO system.

Crystallization activation energy and Avrami parameter

The crystallization kinetics based on thermal analysis (TA) data is usually interpreted in terms of the nucleation growth mechanism formulated by Avrami [33]. According to this model, the fractional crystallization depends on time in the following form:

$$x = 1 - \exp[-(Kt)^n] \quad (1)$$

where K is the effective reaction rate and n an integer, which depends on the mechanism of growth and the dimensionality of the crystal [34]. The effective reaction rate K is given by:

$$K=K_0\exp(-E/RT) \quad (2)$$

where E is the crystallization activation energy and R the ideal gas constant. Equation (2) is generally used as a formal definition for TA crystallization data. When the differential form of Eq. (1) is taken into account, then the Johnson–Mehl–Avrami (JMA) equation can be written as:

$$\left(\frac{dx}{dt}\right) = Kn(1-x)[-\ln(1-x)]^{(n-1)/n} \quad (3)$$

which is frequently used for the formal description of TA crystallization data. But there exist some important points for the validity of JMA equation, at least following conditions should be considered [35–38]; initially isothermal crystallization conditions must be established. One another important point is that the homogeneous nucleation, which is preferable not to fall into error during the calculations of the crystallization data. Also growth ratio of a new phase must be controlled by temperature and should be independent on time and finally low anisotropy of growing crystals is necessary.

Henderson showed that if the entire nucleation process occurs during the early stages of the transformation, JMA equation can be extended to the non-isothermal condition, and solutions of the problems may be done easily [35–37].

Although, some other important methods for calculations of non-isothermal process were also developed by many research groups. For example, a fundamental kinetic method for non-isothermal crystal growth mechanism from the preexisting nuclei has been developed by Ozawa [39]. In this method, mathematical functions were generalized by considering the generalized time concept and widely accepted by the glass-ceramic research groups [28, 32, 35, 40, 41].

Another useful method that is most commonly used in analyzing the TA data, was developed by Kissinger [18]. Kissinger method takes the second derivative of x with respect to time, t, obtains an expression for t and temperature and the peak of the exotherm by equating the second derivative to zero. In this method, by taking the derivative of Eq. (3) with respect to time, it is convenient to assume that near the peak $[-\ln(1-x)]^{(n-1)/n}$ is a constant (denoted A in Eq. (4)) and if the temperature dependence of K is ignored the Eq. (3) can be rewritten in the following form [34]:

$$x=A(1-x)K_0e^{-E/RT} \quad (4)$$

By taking the derivative of Eq. (4),

$$\ddot{x} = AK_0\left(\frac{E}{RT_x^2} - \frac{AK_0}{\alpha}e^{-E/RT_x}\right)\alpha(1-x)e^{-E/RT_x} = 0 \quad (5)$$

or it can be written as:

$$\frac{d\ln(\alpha/T_x^2)}{d(1/T_x)} = -\frac{E_a}{R} \quad (6)$$

where T_x is the first crystallization temperature, α the heating rate, E_a the crystallization activation energy and R the ideal gas constant. If the crystallization mechanism remains constant with the heating rate (α), the plot of $\ln(\alpha/T_x^2)$ *vs*. $1/T_x$ gives a straight line and E_a is calculated from the slope of this line.

Table 2 lists the calculated activation energies and Fig. 3 shows the Kissinger plot for the crystal growth of the samples prepared. The calculated E_a values range from 400 to 434 kJ mol^{-1}. The results obtained showed

Table 2 The crystallization activation energies and Avrami parameters of the samples

x-value	E_a/kJ mol^{-1}	Avrami parameter, n
0.5	400.74	2.48
1.0	434.37	1.71

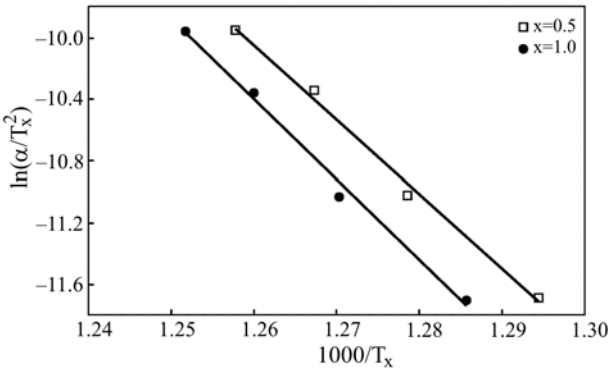

Fig. 3 Kissinger plots of the Er-substituted samples

that the E_a values for Er-substituted system were comparably higher than that of the unsubstituted $Bi_2Sr_2Ca_2Cu_3O_{10+\delta}$ system (E_a=336.46 kJ mol^{-1} in the unsubstituted $Bi_2Sr_2Ca_2Cu_3O_{10+\delta}$ system) [42]. It is well known that the crystallization of a glass system needs the rearrangement of unlike atoms and atoms must overcome the banding energies with neighbors to take its lattice position of primary crystals. This indicates that effective activation energy for crystallization of a glass sample and reflects the interaction of atoms. Therefore, the material containing the substitutional atoms, which show much stronger attractive interaction, produces higher activation energy. It was also noted that the samples prepared in this study show much higher stability than the unsubstituted $Bi_2Sr_2Ca_2Cu_3O_{10+\delta}$ system.

The Avrami parameter, n, can be calculated from the DTA data. The computed value of the n parameter gives the significant information about the crystal morphology of the samples. The Avrami parameter, n, is calculated by using the Ozawa's equation [43]:

$$\frac{d[\ln(-\ln(1-\phi)]}{d(\ln\alpha)} = -n \qquad (7)$$

where α is the heating rate and ϕ is calculated from the ratio of partial area of the crystallization peak at any temperature to the total area of the crystallization peak. The plot of $\ln[-\ln(1-\phi)]$ *vs*. $\ln\alpha$ is obtained to be a straight line, Fig. 4, the slope of this line gives the parameter n.

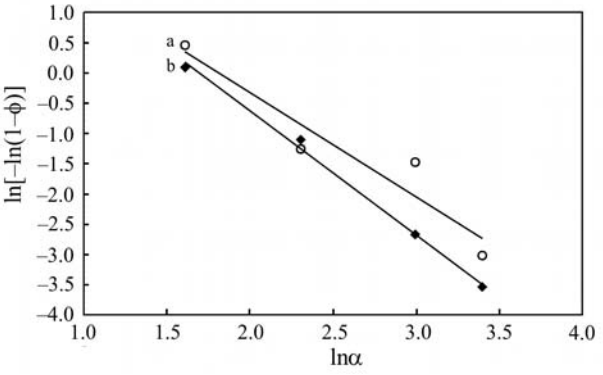

Fig. 4 $\ln(-\ln(1-\phi))$ *vs*. $\ln\alpha$ of a – x=0.5 sample and b – x=1.0 sample

The calculated values of n are listed in Table 2. The n value decreased from 2.5 to 1.7 for x=0.5 and 1.0 samples, respectively. This suggests that the growth mechanism is diffusion-controlled, simultaneous nucleation occurs and three-dimensional parabolic growth takes place in the material during the first crystallization process. In general, for the diffusion-controlled growth, we have the following cases: If n remains between $1.5<n<2.5$, it reflects the growth of small particles with a decreasing nucleation rate, in this case higher activation energy for crystallization demonstrates that atomic diffusion in the material is very difficult. A difficulty in atomic diffusion retards the nucleation and growth process. However, if the n value is higher than 2.5, this indicates growth of small particles with increased nucleation rate [32, 44, 45]. An increase on the nucleation rate results in the compositional fluctuations in the regions adjacent to the growing nuclei, which cause a chain reaction-like process leading to an increase on the nucleation rate.

TG results

TG patterns of the samples taken at heating rate of 10°C min^{-1} in oxygen atmosphere are shown in Fig. 5. In the case of x=0.5 sample, a gradual mass gain started at 356°C due to the oxidization of the samples, Fig. 5a. Obviously, this is necessary for the BSCCO system in order to form the perovskite-type structure. Then a sharp mass gain started at 500°C, Fig. 5a, corresponds to the first exothermic activities obtained in DTA data of this material, Fig. 1b. A stable curve between 608 and 622°C is obtained but then a slight mass loss was observed after 635°C. The mass loss is believed to be due to release of oxygen from the material. The mass increase for this sample is calculated to be 0.792%.

The similar trend was obtained for the x=1.0 sample, Fig. 5b. The mass gain started at 355°C and continued up to 605°C. The mass loss was found at 637°C. The total mass gain was found to be 1.079% which is higher than that of the x=0.5 sample. This indicates that the oxygen absorption of the x=0.5 sample is slower than the x=1.0 sample.

The average oxidization rate was computed using the TG data and results obtained are presented in Table 3. A systematic increase on the average oxidization rate was obtained by increasing the Er-substitution from x=0.5 to 1.0. An increase on the oxidiza-

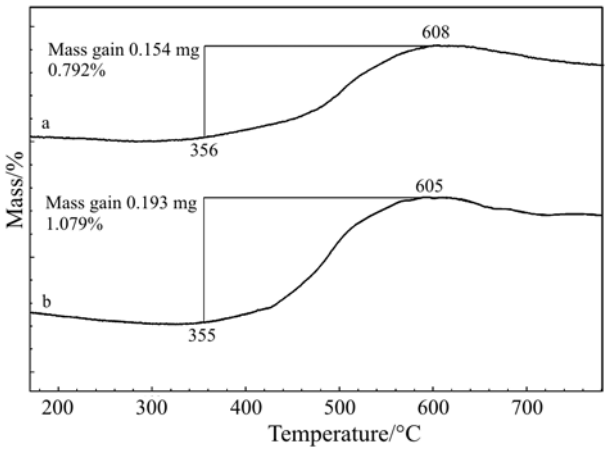

Fig. 5 TG plots of a – x=0.5 and b – x=1.0 samples under O_2 atmosphere

Table 3 The average oxidization rates of x=0.5 and x=1.0 samples. Δm is the total mass increase, $\Delta m/\Delta T$ the mass increase per temperature, $\Delta m/\Delta t$ the mass increase per second, $(\Delta m/\Delta T)/m_{oxygen}$ the mass increase per unit oxygen atom and temperature, and $(\Delta m/\Delta t)/m_{oxygen}$ the mass inrease per unit oxygen atom and second

Sample	Δm/mg	ΔT/°C	$\Delta m/\Delta T$/g °C^{-1}	$\Delta m/\Delta t$/g s^{-1}	$(\Delta m/\Delta T)/m_{oxygen}$/atom °C^{-1}	$(\Delta m/\Delta t)/m_{oxygen}$/atom s^{-1}
x=0.5	0.154	250	$6.16\cdot10^{-7}$	$1.03\cdot10^{-7}$	$2.32\cdot10^{16}$	$3.86\cdot10^{15}$
x=1.0	0.193	252	$7.66\cdot10^{-7}$	$1.28\cdot10^{-7}$	$2.88\cdot10^{16}$	$4.80\cdot10^{15}$

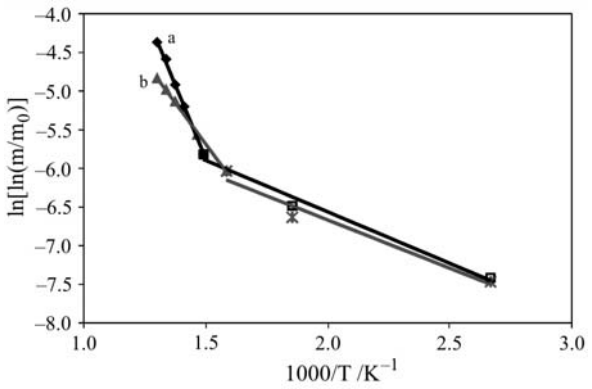

Fig. 6 ln[ln(m/m_0)] *vs.* 1000/T plots for a – x=0.5 sample and b – x=1.0 sample

tion rate indicates that there exist more oxygen deficiencies in the unit cell of the x=1.0 sample compared to the x=0.5 and so more oxygen atoms were absorbed to fill the deficiencies in the material.

The activation barrier for oxygen out-diffusion process can be found using the following equation [46]:

$$\ln\left[\ln\left(\frac{m}{m_0}\right)\right] = -\frac{E}{R}\left(\frac{1}{T}\right) + \text{constant} \qquad (8)$$

where E is the activation barrier for oxygen out-diffusion, m the mass of the material at any given temperature, m_0 the initial mass and R the universal gas constant. Thus, a plot of ln[ln(m/m_0)] *vs*. ln(1/T) yields a straight line that the slope is equal to E/R. Figure 6 shows the plot of ln[ln(m/m_0)] *vs*. ln(1/T). For the x=0.5–Er substituted sample, in the temperature range of 355 and 435°C, the activation barriers, E, was found to be 11.05 kJ mol^{-1} and the temperature range between 435 and 605°C, E was increased to 65.07 kJ mol^{-1}. However, the activation barrier, E, reduced by increasing the Er concentration from x=0.5 to 1.0. The E values were obtained to be 10.31 and 35.50 kJ mol^{-1} for the lower (355–435°C) and higher (435–605°C) temperature ranges, respectively. These results were suggested that the oxygen gain kinetics is faster in the case of x=1.0 sample.

Conclusions

Samples in the nominal composition of $Bi_2Sr_2Ca_2Cu_{3-x}Er_xO_{10+\delta}$, where x=0.5 and 1.0, have been prepared successfully by the glass-ceramic method. The effect of Er on the thermal properties of the Bi-2223 system was investigated. The results obtained showed that the crystallization temperature shifted to the higher temperatures by increasing the Er concentration. This is related with the increase of the surface nucleation in the material. The glass working range, ΔT, is also increased and indicating that glassification improved with the substitution of Er. Higher activation energies for crystallization, E_a, were obtained compared with the unsubstituted BiSrCaCuO materials. The calculated Avrami parameter, n, suggested that crystal growth is diffusion-controlled. An increase on the mass gain was obtained by increasing the Er concentration in the BSCCO system. The activation barrier for oxygen out-diffusion, E, reduced by increasing the Er concentration from x=0.5 to 1.0. This suggested that the oxidization in the x=1.0 sample is faster than that of the x=0.5 sample.

Acknowledgements

This research was supported by Turkish Prime Ministry, State Planning Organization (DPT) under contract no: 2003 K 120610.

References

1 M. D. Ediger, C. A. Angell and S. R. Nagel, J. Phys. Chem., 100 (1996) 13200.
2 B. W. Höland, V. Rheinberger and M. Schweiger, Adv. Eng. Mater., 3 (2001) 768.
3 J. Vázquez, D. Garcia-G. Barreda, P. L. López-Alemany, P. Villares and R. Jiménez-Garay, Mater. Chem. Phys., 86 (2004) 448.
4 J. S. C. Jang, T. H. Hung and L. J. Chang, Mater. Sci. Eng., A (in press).
5 G. Ruitenberg, Thermochim. Acta, 404 (2003) 207.
6 N. Yu. Mikhailenko and N. V. Rudkovskaya, Glass Ceram., 60 (2003) 108.
7 N. Koga and J. Šesták, J. Therm. Anal. Cal., 60 (2000) 667.
8 B. Koscielska, L. Murawski, B. Kusz and L. Wicikowski, Cryst. Res. Technol., 36 (2001) 925.
9 J. Vázquez, P. L. López-Alemany, P. Villares and R. Jiménez-Garay, J. Phys. Chem. Solids, 61 (2000) 493.
10 S. Chatterjee, B. K. Chaudhuri and T. Komatsu, Solid State Commun., 104 (1997) 67.
11 M. Gazda, B. Kusz, S. Chudinov, S. Stizza and R. Natali, Physica, C 387 (2003) 216.
12 M. Gazda, B. Kusz, L. Murawskit, W. Sadowski, S. Fusari, S. Chudinov and S. Stizza, Physica, C 341–348 (2000) 501.

13 B. Koscielska, B. Andrzejewski, W. Sadowski and L. Murawski, Supercond. Sci. Technol., 15 (2002) 1017.
14 M. A. Aksan, M. E. Yakinci and Y. Balci, Supercond. Sci. Technol., 13 (2002) 955.
15 M. A. Aksan and M. E. Yakinci, J. Alloy Compd., 385 (2005) 33.
16 M. A. Aksan, M. E. Yakinci and Y. Balci, J. Supercond., 15 (2002) 553.
17 M. E. Yakinci, I. Aksoy and M. Ceylan, J. Mater. Sci., 31 (1996) 2865.
18 H. E. Kissinger, J. Res. Natl. Bur. Stand., 57 (1956) 217.
19 T. Komatsu, R. Sato, C. Hirose, K. Matusita and T. Yamoshita, Jpn. J. Appl. Phys., 27 (1988) L2293.
20 Y. Balci, M. Ceylan and M. E. Yakinci, Mater. Sci. Eng., B., 86 (2001) 83.
21 Z. Ozhanli, M. E. Yakinci, Y. Balci and M. A. Aksan, J. Supercond., 15 (2002) 543.
22 M. E. Yakinci, I. Aksoy and A. Ozdes, Physica, C 235–240 (1994) 959.
23 P. Somasundaram and A. M. Umarji, Physica, C 209 (1993) 393.
24 D. Shi, M. Tang, M. S. Boley, M. Hash, K. Vandervoort, H. Claus and Y. N. Lwin, Phys. Rev., B 40 (1989) 2247.
25 M. R. De Guire, N. P. Bansal and C. J. Kim, J. Am. Ceram. Soc., 73 (1990) 1165.
26 R. Sato, T. Komatsu and K. Matusita, J. Mater. Sci. Lett., 10 (1991) 355.
27 C. H. Hwang and G. Kim, Supercond. Sci. Technol., 5 (1992) 586.
28 C. H. Shan and S. H. Risbud, Supercond. Sci. Technol., 6 (1993) 736.
29 P. E. Kazin, V. V. Poltavets, Y. D. Tretyakov, M. Jansen, B. Freitag and W. Mader, Supercond. Sci. Technol., 12 (1999) 475.
30 T. Komatsu, R. Sato, H. Meguro, K. Matusita and T. Yamashita, J. Mater. Sci., 26 (1991) 683.
31 Y. Dimitriev, B. Samuneva, Y. Ivanova, E. Gattef, V. Mihailova and A. Staneva, Supercond. Sci. Tech., 3 (1990) 606.
32 A. Karamanov and M. Pelino, J. Non-Cryst. Solids, 290 (2001) 173.
33 M. Avrami, J. Chem. Phys., 7 (1939) 1103.
34 H. Yinnon and D. R. Uhlmann, J. Non-Cryst. Solids, 54 (1983) 253.
35 J. Malek, Thermochim. Acta, 355 (2000) 239.
36 D. W. Henderson, J. Thermal Anal., 15 (1979) 325.
37 D. W. Henderson, J. Non-Cryst. Solids, 30 (1979) 301.
38 M. P. Shepilov and D. S. Baik, J. Non-Cryst. Solids, 171 (1994) 141.
39 T. Ozawa, Bull. Chem. Soc. Jpn., 57 (1984) 639.
40 S. Kurajica, A. Bezjak and E. Tkalcec, Thermochim. Acta, 360 (2000) 63.
41 A. Karamanov, P. Pisciella and M. Pelino, J. Eur. Ceram. Soc., 20 (2000) 2233.
42 Y. Balci, Crystallization kinetics of glass-ceramics superconductors and investigation of the electrical conductivity properties, PhD Thesis, Firat University, Elaziğ, Turkey 1997.
43 T. Ozawa, Polymer, 12 (1971) 150.
44 J. W. Christian (Ed.), The Theory of Transformation in Metals and Alloys, Pergamon Press, Oxford 1975.
45 Z. J. Yan, S. R. He, J. R. Li and Y. H. Zhou, J. Alloys Compd., 368 (2004) 175.
46 A. Broido, J. Polym. Sci. Part A-2, 7 (1969) 1761.

Received: October 16, 2004
In revised form: January 10, 2005

DOI: 10.1007/s10973-005-6554-6